Modeling of a Monolithic Catalyst with Reciprocating Flow

K. Wallace and H. J. Viljoen
Dept. of Chemical Engineering, University of Nebraska, Lincoln, NE 68588

Several methods have been proposed to improve the conversion of catalytic oxidation reactions. Gases with low enthalpy contents or gases that contain small amounts of combustible compounds can be converted much more efficiently in a reactor with reciprocating flow. The solid phase exhibits an inertia behavior insofar as it does not reach equilibrium with the gas temperature at the reactor ends. The solid-phase temperature at the center of the bed is considerably higher than in the unidirectional case. Results for the oxidation of CO at different inlet gas temperatures and switching periods are presented. An optimum period is found at which maximum conversion occurs. An estimate of the maximum temperature in the reactor is derived.

Introduction

Monolithic catalysts are widely used for the control of air pollution. Since the inception of this technology, certain shortcomings have been recognized, in particular the heat-and mass-transfer limitations. Some imaginative solutions have been proposed to improve mass transfer. Wendland (1980) proposed a segmented system. Multiple pieces of monolith were placed in series. The flow became turbulent between sections, and every section had its own developing entry lengths where mass- and heat-transfer coefficients were larger. The system has been tested under laboratory conditions and improved conversions have been measured. In a more recent study, Psyllos and Philippopoulos (1993) proposed to grade the catalyst concentration through the reactor. The results of their numerical study showed that the conversion improved under certain conditions when the metal catalyst concentration was axially distributed. A parabolic profile of catalyst density (g/cm^2) with the minimum at the center was shown to outperform reactors with a constant density distribution. Andersson and Schoon (1993) used a three-dimensional flow model to study the effect of obstacles in the channel on the catalyst performance. Increased reduction in CO varied between 33 and 44%, but at the expense of increased pressure drop.

Exhaust streams with low combustible contents cannot light-off or sustain the reaction in the ignited state without additional heating. An interesting solution is to reciprocate the flow through the monolith. Matros (1990) reported on theoretical and experimental studies of fixed bed catalytic reactors that were operated with reciprocating flow. These reactors were used for the processing of gases with low concentrations of the reacting components. Gases with adiabatic temperature rises as low as 10–15°C were reacted without additional preheating. These findings were consistent with more recent results of Hanamura et al. (1993). They designed and operated a porous burner with reciprocating flow. They were able to raise the solid-phase temperature in the burner to more than 13 times the adiabatic temperature rise. Eigenberger and Nieken (1988) did a numerical and experimental investigation of the combustion of a propene–methane–air mixture in a monolithic catalyst with reciprocating flow. They considered a pseudohomogeneous model with first-order kinetics and found that the maximum temperature in the bed decreased with increasing values of the activation energy and the rate constant. Rehacek et al. (1992) analyzed the two-phase problem with reciprocating flow. Conduction in both phases, as well as diffusion in the gas phase, were included. An interesting result of that study was the existence of asymmetric solutions. Even windows of aperiodic temporal behavior were found.

In this theoretical study we investigate the performance of a monolith catalyst with reciprocating flow. The oxidation of CO is used as the working example. Radiation and axial conduction are included in the solid-phase energy balance, but conduction and diffusion are neglected in the gas phase. An expression is derived for the maximum temperature in the solid phase. As far as the practical implementation is concerned, this flow arrangement has already been demon-

Correspondence concerning this article should be addressed to H. J. Viljoen.

strated in fixed-bed reactors (Matros, 1990; Blanks et al., 1990) and in porous burner systems by Yoshida et al. (1984), Hanamura et al. (1993), and Min and Shin (1991).

The Model

Consider a single channel of a monolithic honeycomb converter. The channel has a length L, diameter D, and wall thickness Δt. The following equations describe the species and temperature balances.

$$\frac{\partial C_{fo}}{\partial t} + U\frac{\partial C_{fo}}{\partial x} = -\sigma\frac{k_c}{S_f}[C_{fo} - C_{wo}] \tag{1}$$

$$\frac{\partial C_{fc}}{\partial t} + U\frac{\partial C_{fc}}{\partial x} = -\sigma\frac{k_c}{S_f}[C_{fc} - C_{wc}] \tag{2}$$

$$\frac{\partial T_f}{\partial t} + U\frac{\partial T_f}{\partial x} = -\sigma\frac{k_H}{S_f\rho_f Cp_f}[T_f - T_w] \tag{3}$$

$$\frac{\partial T_w}{\partial t} - \kappa_w\frac{\partial^2 T_w}{\partial x^2} = \frac{k_H}{\rho_w Cp_w \Delta t}[T_f - T_w] + \frac{(-\Delta H)k_o}{\Delta t\rho_w Cp_w}\frac{C_{wo}C_{wc}e^{-E/RT_w}}{(1+k_1C_{wc})^2} - \frac{Q_R}{\Delta t\rho_w Cp_w} \tag{4}$$

$$k_c(C_{fc} - C_{wc}) = k_o\frac{C_{wo}C_{wc}e^{-E/RT_w}}{(1+k_1C_{wc})^2} \tag{5}$$

$$k_c(C_{fo} - C_{wo}) = \frac{k_o}{2}\frac{C_{wo}C_{wc}e^{-E/RT_w}}{(1+k_1C_{wc})^2}. \tag{6}$$

The first two equations describe the oxygen and carbon monoxide balances in the gas phase. The energy balance in the gas phase is given by Eq. 3. Convection and heat transfer between the gas and solid phases are considered. Equation 4 describes the energy balance of the solid phase. Conduction is included, as well as radiation through the presence of the radiation flux term Q_R. The heat of reaction also contributes to the energy balance. Equations 5 and 6 describe the equilibrium between mass transfer to the surface and the reaction rate. The contribution of radiation to the energy transfer is given by the net radiative heat flux governed by the radiative transfer equation (cf. Min and Shin, 1991):

$$\frac{d^2Q_R}{dx^2} - \frac{4\epsilon}{D^2}Q_R = \epsilon\frac{d^2E_s}{dx^2} \tag{7}$$

where E_s is the total hemispherical emissive power,

$$E_s = \sigma_B T_w^4. \tag{8}$$

The system is closed by the following set of initial and boundary conditions:

$$C_{fo} = C_{foi} \tag{9}$$

$$C_{fc} = C_{fci} \tag{10}$$

$$T_f = T_{fi} \tag{11}$$

$$\frac{dT_w}{dx} = 0, \quad x = 0, L. \tag{12}$$

$$\frac{dQ_R}{dx} - \frac{2}{D}Q_R = \epsilon\left[\frac{dE_s}{dx} - \frac{2}{D}(E_s - E_{\text{in}})\right], \quad x = x_{\text{in}} \tag{13}$$

$$\frac{dQ_R}{dx} + \frac{2}{D}Q_R = \epsilon\left[\frac{dE_s}{dx} + \frac{2}{D}(E_s - E_{\text{out}})\right], \quad x = x_{\text{out}}. \tag{14}$$

The boundary conditions for the radiative transfer equation include radiation from surfaces upstream or downstream of the reactor (E_{in} and E_{out}). These boundary conditions change when the flow direction is switched and the boundaries are denoted as x_{in} and x_{out}.

The Nusselt number for heat transfer was estimated as follows. The Reynolds number upstream of the reactor is usually large (cf. Heck et al., 1976), and it is assumed that the flow is turbulent. Upon entering the channel, the flow develops both hydrodynamically and thermally. Langhaar (cf. Knudsen and Katz, 1958) analyzed the hydrodynamic development of an isothermal fluid, and Kay (cf. Knudsen and Katz, 1958) used that solution in the Graetz problem to determine the local Nusselt number Nu_x. Taking $Pr = 0.7$, relationships for Nu_x were developed based on conditions of constant heat flux, temperature difference, and wall temperature (cf. Knudsen and Katz, 1958). None of these three conditions was exactly satisfied in our case, but Heck et al. (1976) have found that the local Nusselt number followed a constant flux relationship prior to light-off and a constant wall-temperature relationship after light-off occurred. Votruba et al. (1975) correlated Nusselt $Re\ (D/L)$ data and proposed the following relationship: $Nu = 0.571(Re(D/L)^{2/3}$. This relationship, however, did not describe inlet behavior. The importance of enhanced heat- and mass-transfer coefficients at the inlet was demonstrated by Wendland (1980) in a series of experiments. He showed that the conversion in segmented converters was considerably better than in single-stage reactors, with an average 47% improvement in the fraction of unconverted CO. He correlated experimental measurements of Hornbeck (see Wendland, 1980) to describe the local nature of the heat- and mass-transfer coefficients near the inlet. The experimental results of Wendland led us to believe that the inlet effect diminishes more slowly than indicated by the theoretical results of Kay (Knudsen and Katz, 1958). Instead, we used the same data as Wendland, which were correlated as

$$Nu = 3.66\left[1 + \frac{0.05226}{\dfrac{\xi}{Pe_f\dfrac{D}{L}} + 0.0166}\right]. \tag{15}$$

The mass-transfer coefficient was evaluated from the following relation, proposed by Votruba et al. (1975):

$$Sh = 0.705\left[Re\frac{D}{L}\right]^{0.43}Sc^{0.56}. \tag{16}$$

We now introduce L and (L/U) as scales for length and time. The following dimensionless temperatures, radiation flux, and concentrations are defined:

$$\theta_m = \frac{T_m - T_{fi}}{T_{fi}}, \qquad q_R = \frac{Q_R}{\sigma_B T_{fi}^4}, \qquad c_{mn} = \frac{C_{mn}}{C_{fni}},$$

where $m \equiv f, w$ and $n \equiv c, o$. The dimensionless forms of the governing equations are written as

$$\frac{\partial c_{fo}}{\partial \tau} + u\frac{\partial c_{fo}}{\partial \xi} = -\beta_1[c_{fo} - c_{wo}] \tag{17}$$

$$\frac{\partial c_{fc}}{\partial \tau} + u\frac{\partial c_{fc}}{\partial \xi} = -\beta_1[c_{fc} - c_{wc}] \tag{18}$$

$$\frac{\partial \theta_f}{\partial \tau} + u\frac{\partial \theta_f}{\partial \xi} = -\beta_2[\theta_f - \theta_w] \tag{19}$$

$$\frac{\partial \theta_w}{\partial \tau} - \frac{1}{Pe_w}\frac{\partial \theta_w}{\partial \xi^2} = \beta_5[\theta_f - \theta_w] + \frac{\beta_3\beta_5 Da_2 c_{wo} c_{wc} e^{\gamma\theta_w/1+\theta_w}}{(1+\kappa_1 c_{wc})^2} - \beta_4 q_R \tag{20}$$

$$C_{fo} - c_{wo} = \frac{Da_2}{2}\frac{c_{wo} c_{wc} e^{\gamma\theta_w/1+\theta_w}}{(1+\kappa_1 c_{wc})^2} \tag{21}$$

$$c_{fc} - C_{wc} = Da_1 \frac{c_{wo} c_{wc} e^{\gamma\theta_w/1+\theta_w}}{(1+\kappa_1 c_{wc})^2}. \tag{22}$$

The dimensionless velocity u is defined as

$$u = \text{sign}\left[\cos\left(\frac{2\pi\tau}{\omega}\right)\right]. \tag{23}$$

The switching period is ω (if P denotes the period in real time, then $\omega = PU/L$).

Results

The set of dimensionless equations was discretized using finite differences. This initial-value problem was solved, using explicit integration with adjustable time step. The grid was refined (equidistant) by doubling the existing number of grid points, say N. Once the maximum of the absolute differences in the dimensionless wall temperatures at the N points was less than 10^{-3}, the grid was used in further calculations.

The results of the reciprocating flow cases are compared with the results for unidirectional flow. The switching period ω is varied, and its effect on the outlet concentration and maximum temperature is studied. Different inlet gas temperatures are considered. In Table 1 the parameter values used in this study are listed.

Switching period

The inlet gas temperature is fixed at 500 K for all the results presented in this section. The outlet concentration for unidirectional flow is 6.88% (of inlet value), and the maximum temperature in the solid phase of 692 K is reached at the outlet. The time-averaged outlet concentrations for the switching periods of 200, 150, and 100, are 4.34, 3.31, and 5.10%, respectively. The maximum temperatures for the three different switching periods (200, 150, and 100) vary from 900 K, 927 K to 910 K. By switching, the system's temperature far exceeds the unidirectional feed temperature. Of course, one cannot raise the temperature without consideration for physical limitations like sintering of the catalyst or phase transformations of the support. At $\omega = 150$, the outlet concentration has halved, compared to the unidirectional case. The existence of a local optimum of ω is apparent from these results. Considering the fact that the $\lim_{\omega\to\infty} c_{wc}(x_{\text{out}})$ is the same as the outlet concentration for unidirectional flow, and the $\lim_{\omega\to 0} c_{wc}(x_{\text{out}}) = 1$, this is not an unexpected result. The best conversion is obtained at $\omega = 150$, although this value can be further refined.

In Figure 1 the wall temperature at the outlet is plotted as a function of time for $\omega = 200$. The peak values differ from one cycle to the other, that is, the wall temperature at $x = 0$ is not mirrored at $x = 1$ during the second half of the period. The temperature profile in the solid phase has a parabolic shape and the maximum is located near the center. At startup an asymmetric profile is established over the first half-period, since the unidirectional solution is approached. Switching changes the direction of the thermal wave, but the asymmetry persists. Consider a cycle with the inlet flow at $x = 0$. The temperature of the solid phase decreases near the inlet due to heat transfer to the gas phase, but it does not reach the same temperature as the inlet gas stream. When the flow is switched, the solid phase close to $x = 0$ (now at the outlet) is in contact with the combusted gas (heated at the center) and it is heated to a higher temperature. As long as the outlet gas temperature is below the adiabatic temperature, the solid-phase temperature will continue to rise. An interesting analogy exists between this system and the behavior of the positive-ion cloud in an RF glow discharge that also exhibits inertia toward the varying electric field.

Table 1. Parameter Values

Item	Units	Value/Expression
ν_f	m^2/s	$(-37.45+0.15T_{fi})\times 10^{-6}$
ρ_f	kg/m^3	$342/T_{fi}$
$\rho_f Cp_f$	$J/m^3\cdot K$	$0.014/\nu_f$
ρ_w	kg/m^3	2,500
Cp_w	$J/kg\cdot K$	1,225
C_{tot}	mol/m^3	$12{,}214.29/T_{fi}$
C_{fci}	mol/m^3	$0.01\times C_{tot}$
C_{foi}	mol/m^3	$0.01\times C_{tot}$
D	m	0.00126
k_o	$m^4/mol\cdot s$	$(4.14\times 10^{11})/C_{tot}^2$
E/R	K	12,600
L	m	0.1016 (base case)
T_{fi}	K	450/500/600
$-\Delta H$	J/mol	2.8×10^5
Π	Pa	101,325
D_f	m^2/s	$\nu_f/0.72$
ϵ		0.4
k_f	$W/m\cdot K$	0.05
k_w	$W/m\cdot K$	27

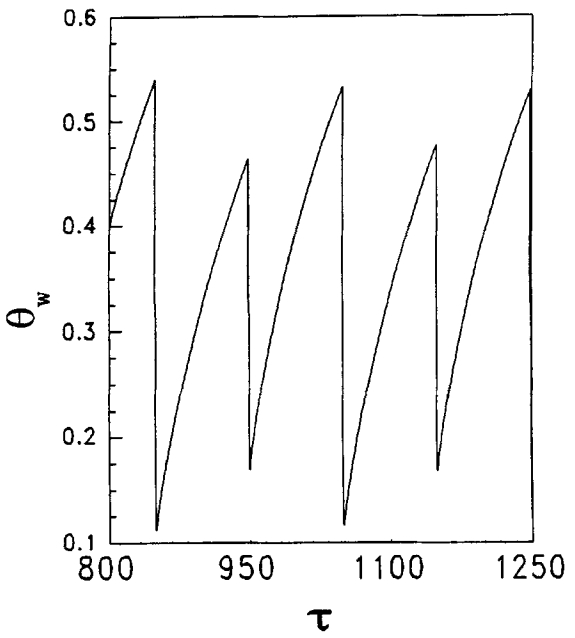

Figure 1. Outlet wall temperature vs. time for $\omega = 200$.

In Figure 2 the outlet CO concentration (c_{fcout}) is plotted as a function of time. The switching period is $\omega = 100$. The peaks coincide with the half-period, and at the moment of switching the peak has the same value as the inlet CO concentration. But the concentration drops off very sharply, dipping slightly below the equilibrium value. The reason for this is that a pocket of lower-concentration gas (which has formerly been near the outlet during the previous cycle) is flowing through the reactor, and it has a lower outlet concentration. For most of the cycling period, the reaction is mass-transfer controlled. The temperature does not reach a steady state during a cycle. In contrast, the concentration distribution reaches an equilibrium shortly after switching has taken place. When the flow reciprocates, the maximum temperature is located near the center of the reactor. As the period is extended, the slow thermal wave in the solid phase travels further downstream (similar to a pendulum) over a half-period. Rehacek et al. (1992) reported similar results.

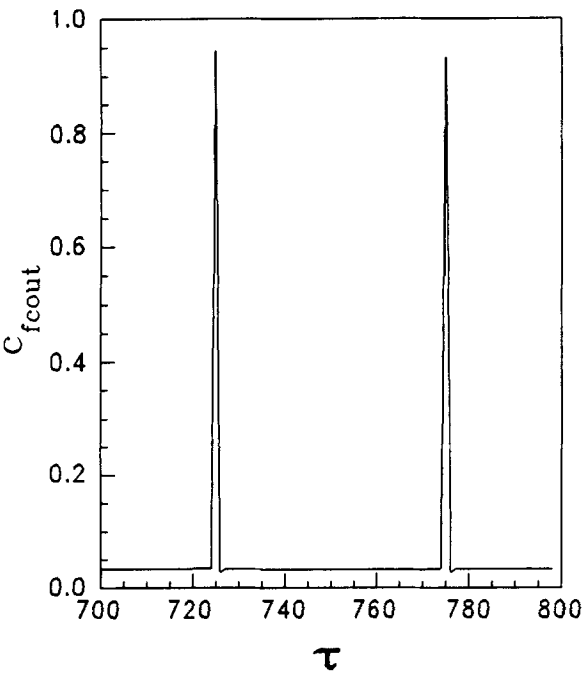

Figure 2. Outlet CO concentration vs. time, at $\omega = 100$.

Inlet temperature

In this section, the switching period in cases of reciprocating flow is fixed at $\omega = 150$. Differences in conversion between the reciprocating and unidirectional flow operations diminish when the inlet temperature is increased. Mass-transfer limitations begin to play an increasingly important role, and at higher inlet temperatures all kinetic limitations disappear. At an inlet temperature of 500 K, the mean outlet concentration for reciprocating flow is 3.31%, compared to 6.88% for unidirectional flow. When the inlet temperature is increased to 600 K, the respective values are 2.42 and 2.48 %. Another aspect one should keep in mind is the changes in physical properties with changes in inlet temperature. We do not consider variable physical properties throughout the reactor, but they depend on the inlet temperature (see also Table 1).

When the inlet temperature is lowered to 450 K, the unidirectional system is unable to light-off and the conversion drops to 2.5% (outlet concentration 97.5% of inlet). On the other hand, the reciprocating system accumulates enough energy to maintain an average outlet concentration of 4.79%.

Estimation of maximum temperature

It would be useful to have an explicit expression for the maximum temperature in the reactor; ideally, one would like to find an upper bound on the temperature. To our knowledge a constructive proof of the existence of such a bound for a mixed hyperbolic–parabolic problem does not exist (cf. Protter and Weinberger, 1967), nor will such a proof be trivial. However, an estimate of the maximum temperature in the reactor can be derived as follows. The first step is to find an upper bound on the reaction term. For the stoichiometric case or the case where CO is the limiting species, it follows from Eq. 22 that

$$c_{wc} = \frac{c_{fc}}{1 + Da_1 \dfrac{c_{wo} e^{\gamma\theta_w/1+\theta_w}}{(1+\kappa_1 c_{wc})^2}} \leq \frac{c_{fc}}{Da_1 \dfrac{c_{wo} e^{\gamma\theta_w/1+\theta_w}}{(1+\kappa_1 c_{wc})^2}}. \tag{24}$$

Remark: If O_2 is the limiting species, choose Eq. 21 instead.

Inequality (Eq. 24) holds under all conditions, and hence the reaction term can be bounded from above as follows:

$$Da_1 \frac{c_{wc} c_{wo} e^{\gamma\theta_w/1+\theta_w}}{(1+\kappa_1 c_{wc})^2} \le c_{fc}.$$

Furthermore, we use the fact that the concentration profiles are in a quasi-steady state most of the time (a result of the short characteristic time of reaction and $P \gg L/U$). Considering the steady-state form of Eq. 19, it can integrated to give

$$c_{fc} = \begin{cases} e^{-\beta_1 \xi} & \text{if } u > 0 \\ e^{-\beta_1(1-\xi)} & \text{if } u < 0. \end{cases}$$

Now we have an explicit expression for the upper bound on the reaction rate. The energy balances can be written as

$$\frac{\partial\theta_f}{\partial\tau} = -u \frac{\partial\theta_f}{\partial\xi} - \beta_2[\theta_f - \theta_w] \tag{25}$$

$$\frac{\partial\theta_w}{\partial\tau} \le \frac{1}{Pe_w} \frac{\partial\theta_w}{\partial\xi^2} + \beta_5[\theta_f - \theta_w] + \frac{\beta_3 \beta_5 Da_2}{Da_1} c_{fc}. \tag{26}$$

Note: We are neglecting the role of radiation in this estimation.

Numerical results indicate that the maximum temperature is located at the center of the bed. Admittedly we have been led by the numerical results, but formally we assume that the maximum temperature is at the center. The maximum is only slightly displaced from the center over a half-period, because it moves very slowly on the time scale that the system is forced; the speed at which a thermal wave propagates through the solid phase is much smaller than L/P. We solve the steady-state forms of Eqs. 25 and 26 at the center of the reactor. In order to do this, the operator $[d^2/d\xi^2]$ is approximated (locally) by $\{-k^2.\}$, an approximation that has been applied successfully by Hlavacek and Hofmann (1970) and Viljoen et al. (1988). These approximations of linear operators are found in weighted residual methods. The different methods produce slightly different values for k^2. It follows from Eq. 25 that

$$\theta_f(0.5) = \theta_w(0.5).$$

Using inequality 26, the maximum temperature is bounded from above as follows

$$\theta_{w\max} \le \frac{\beta_3 \beta_5 Da_2 Pe_w c_{fc}(0.5)}{Da_1 k^2}. \tag{27}$$

What is of more interest is the information about the effect of parameters like the length of the reactor on the maximum. Let F denote the righthand side (r.h.s.) of inequality (Eq. 27). Although $\theta_{w\max} \le F$, we will continue to use the functional form of F to extract some information about $\theta_{w\max}$ itself. Substituting the dimensionless parameters in F in terms of the original physical parameters, the following relationship is found between the parameters and the estimated maximum:

$$F = \frac{C_{fci}(-\Delta H) C_{foi} k_c}{T_{fi} \pi^2 \rho_w C p_w \Delta t \kappa_w} L^2 \exp^{-2k_c L/DU} \tag{28}$$

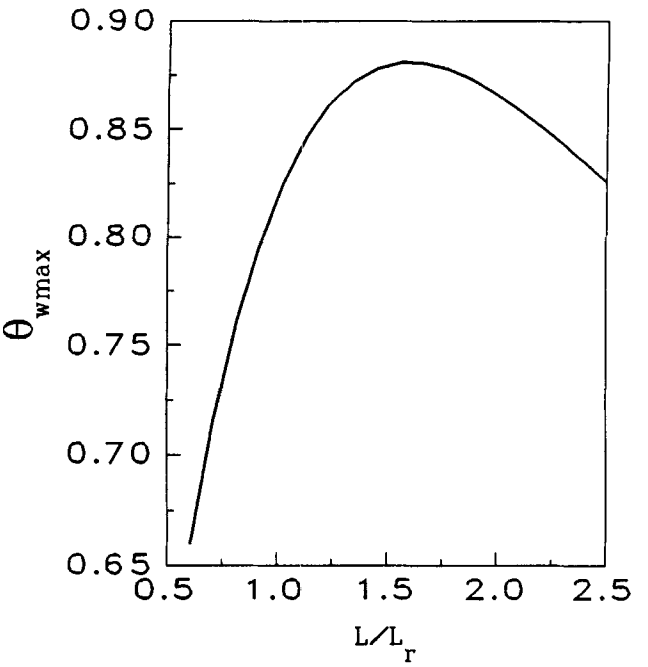

Figure 3. Max $\theta_w(\xi, \tau)$ vs. L at $\omega = 50$.

It is obvious that there exists a length where $\theta_{w\max}(L)$ is maximized. The existence of an optimum length (to maximize $\theta_{w\max}(L)$) is checked numerically by solving the governing Eqs. 18–23. The inlet temperature is 500 K, and the switching period is $w = 50$. All the parameters of the model are constant, except those that depend on L. The reference length L_r is 0.1016 m (Table 1). In Figure 3 the maximum temperature $\theta_{w\max}$ is plotted as a function of length, L/L_r. A maximum is found at $L/L_r \approx 1.6$. Similar relations can be drawn between $\theta_{w\max}$ and some other parameters (such as $\theta_{w\max}(k_c)$.

Since we have used an upper bound on the reaction rate that contains only the mass-transfer coefficient and velocity, the roles of activation energy and rate constants are not described by inequality (Eq. 27) (see Eigenberger and Nieken, 1988). The maximum temperature has a monotonic dependence on velocity. This is somewhat misleading, since the reaction term has been substituted by c_{fc}, which depends on the rate of convection (U). Therefore the estimate reflects a relationship $(\partial\theta_{w\max}/\partial U) > 0$, but it only holds when the system is mass-transfer controlled. If the system is mass-transfer controlled, there are two reasons to expect an increase in temperature with increasing velocity. The first reason is the higher concentration, as we have already discussed. The second reason is that the correlations for heat and mass-transfer coefficients are usually proportional to the Reynolds number, raised to some positive power. Although the analysis cannot be considered as general, it offers additional insight into the problem and should stimulate further research.

Conclusions

A model for the catalytic oxidation of CO in a monolith has been described. At low inlet gas temperatures or low reactant concentrations, the reciprocating system performs much better than the unidirectional system and the reactor

can reach temperatures that are well above the adiabatic temperature. The elevated bed temperature eliminates kinetic limitations in the reactor. The conversion can be improved considerably by optimizing the switching period. This optimum is reached when the reciprocating flow has effectively eliminated the kinetic limitations, but the period is long enough to minimize the emission of pockets of unreacted gas when the flow is switched (see the spikes in Figure 2). As the inlet temperature is lowered, the unidirectional system extinguishes first. The reciprocating system can sustain an ignited state over a wider range of inlet temperatures. An estimate for the maximum temperature has also been derived. Lower thermal conductivity of the solid phase, higher velocities, and higher inlet concentration of CO will all lead to higher maximum temperatures. Kinetic parameters do not appear in the estimate for $\theta_{w\max}$ since the reaction term is substituted for c_f.

Notation

A = constant
B = constant
C = concentration
C_p = specific heat
$Da_1 = (k_o C_{foi})/k_c$
$Da_2 = (k_o C_{fci})/k_c$
D_f = diffusion coefficient
E = activation energy
$(-\Delta H)$ = heat of reaction
k_c = mass-transfer coefficient
k_H = heat-transfer coefficient
$k_{f,w}$ = thermal conductivity
k_o = frequency factor
$Pe_{f,w}$ = Peclet number $UL/k_{f,w}$
q_R = dimensionless radiation flux $Q_R/\sigma_B T_{fi}^4$
R = universal gas constant
Re = Reynolds number $(\rho_f DU)/\mu_f$
Sc = Schmidt number $\mu_f/(\rho_f D_f)$
$S_f = \pi D^2/4$
Sh = Sherwood number $(k_c D)/D_f$
T = temperature
t = time
U = velocity
x = axial distance

Greek letters

$\beta_1 = (\sigma k_c L)/S_f U$
$\beta_2 = (\sigma k_H L)/(S_f \rho_f C p_f U)$
$\beta_3 = [(-\Delta H) C_{foi} k_c]/(k_H T_{fi})$
$\beta_4 = (\sigma_B T_{fi}^4 L)/(\rho_w C p_w U \Delta t)$
$\beta_5 = (k_H L)/(U \rho_w C p_w \Delta t)$
$\gamma = E/(RT_{fi})$
ϵ = emissivity
$\kappa_1 = k_1 C_{fci}$
$\kappa_w = k_w/(\rho_w C p_w)$
μ_f = dynamic viscosity
ν = dimensionless velocity of thermal wave in solid phase
ν_f = kinematic viscosity
ξ = dimensionless spatial variable x/L
ω = dimensionless period $(PU)/L$
Π = mean pressure in reactor
ρ = density
$\sigma = \pi D$
σ_B = Stefan-Boltzmann constant
τ = dimensionless time tU/L
θ = dimensionless temperature

Subscripts

c = CO species
f = gas phase
i = inlet condition
o = O_2 species
r = reference value
w = solid phase

Literature Cited

Andersson, S. L., and N.-H. Schoon, "Methods to Increase the Efficiency of a Metallic Monolithic Converter," *Ind. Eng. Chem. Res.*, **32**, 1081 (1993).

Blanks, R. R., T. S. Wittrig, and D. A. Peterson, "Bidirectional Adiabatic Synthesis Gas Generator," *Chem. Eng. Sci.*, **45**, 2407 (1990).

Eigenberger, G., and U. Nieken, "Catalytic Combustion with Periodic Flow Reversal," *Chem. Eng. Sci.*, **43**, 2109 (1988).

Hanamura, K., R. Echigo, and S. A. Zhdanok, "Superadiabatic Combustion in a Porous Medium," *Ind. J. Heat Mass Transfer*, **36**, 3201 (1993).

Heck, R. H., J. Wei, and J. R. Katzer, "Mathematical Modeling of Monolithic Catalysts," *AIChE J.*, **22**, 477 (1976).

Hlavacek, V., and H. Hofmann, "Modeling of Chemical Reactors XVI. Steady State Axial Heat and Mass Transfer in Tubular Reactors. An Analysis of the Uniqueness of Solutions," *Chem. Eng. Sci.*, **25**, 173 (1970).

Knudsen, J. G., and D. L. Katz, *Fluid Dynamics and Heat Transfer*, McGraw-Hill, New York (1958).

Matros, Yu. Sh., "Performance of Catalytic Processes under Unsteady Conditions," *Chem. Eng. Sci.*, **45**, 2097 (1990).

Min, D. K., and H. D. Shin, "Laminar Premixed Flame Stabilized Inside a Honeycomb Ceramic," *Int. J. Heat Mass Transfer*, **34**, 341 (1991).

Psyllos, A., and C. Philippopoulos, "Performance of a Monolithic Catalytic Converter Used in Automotive Emission Control: The Effect of a Longitudinal Parabolic Active Metal Distribution," *Ind. Eng. Chem. Res.*, **32**, 1555 (1993).

Protter, M. H., and H. F. Weinberger, *Maximum Principles in Differential Equations*, Prentice-Hall, Englewood Cliffs, NJ (1967).

Rehacek, J., M. Kubicek, and M. Marek., "Modelling of a Tubular Catalytic Reactor with Flow Reversal," *Chem. Eng. Sci.*, **47**, 2897 (1992).

Viljoen, H. J., J. E. Gatica, and V. Hlavacek, "Induction Times for Thermal Explosion and Natural Convection in Porous Media," *Chem. Eng. Sci.*, **43**, 2951 (1988).

Votruba, J., O. Mikus, K. Nguen, V. Hlavacek, and J. Skrivanek, "Heat and Mass Transfer in Monolithic Honeycomb Catalysts II," *Chem. Eng. Sci.*, **30**, 201 (1975).

Wendland, D. W., "The Segmented Oxidizing Monolith Catalytic Converter," *Trans. ASME*, **102**, 194 (1980).

Yoshida, H., J. H. Yun, R. Echigo, and T. Tomimura, "Transient Characteristics of Combined Conduction, Convection and Radiation Heat Transfer in Porous Media," *Int. J. Heat Mass Transfer*, **33**, 847 (1990).

Manuscript received Mar. 21, 1994, and revision received June 27, 1994.